



# 3D Prediction of the Wake Rotor of Horizontal Axis Wind Turbines

Noura Belkheir<sup>1</sup>, Ivan Dobrev<sup>2</sup> and khelladi Sofiane<sup>2</sup>

<sup>1</sup>Laboratory FIMA University of Djillali Bounaama Khemis Miliana, Algeria

<sup>2</sup>Arts et Métiers Paris Tech Paris, France

\*Corresponding author E-mail: [nourabelhadj@yahoo.fr](mailto:nourabelhadj@yahoo.fr)

## Abstract

The investigation of the wake development of the wind turbines is important for the wind turbine design, in this paper a modeling of a complete rotor of three blades was implemented to investigate the wake downstream of a wind turbine with horizontal axis. The rotor modeled studied here is a commercial wind turbine i.e. Rutland 503 of the Marlec Company.

The numerical simulations are made for many different tip speed ratio, these are chosen in reference to experimental work realized in the laboratory of ENSAM. The Numerical results were obtained, using the approach Reynolds Averaged Navier Stokes (URANS) equations, the turbulence model used is the Shear Stress Transport (SST)  $k-\omega$ .

The solutions are obtained by using the package FLUENT solver, who uses finite volume method. The wake characteristics of the rotor are compared with the experimental data. The results presented the development of the downstream wake of the wind turbine rotor.

These results provide a good understanding of the unsteady flow in a wind turbine, which will be used to better optimize wind turbine structures and increase the number of wind turbines in wind farms.

**Keywords:** Wind Turbine –wake– URANS Simulation – SST model.

## 1. Introduction

Due to the increasing demand for energy and a high cost of oil energy, there has been a rapid development of wind turbines. In order to minimize the cost of the electric energy production of the wind turbines, they are grouped in farms. The distance between the machines is reduced. So, Wind turbines installed in a wind farm pose aerodynamic interaction problems. Generally, the positioning of wind turbines in the wind farm is a complex problem. Much software was developed for the design of the wind farms is used. This software mainly takes into account the wake of the wind turbines, the speed and direction of the winds and the topography of the site.

The flow around the wind turbine rotor is very complex and it is very difficult to obtain the velocity field of down-stream wake. Turbine wake characteristics depend on many factors, wind speed, turbulence, site topography and the turbine characteristics [1].

Approaches experimental are available to analyze the flow around and downstream of a wind turbine: which provides accurate results but is highly complex, expensive and limited in a spatial and temporal resolution.

In the same, the analytical and semi-empirical models, which adopt simplifying assumptions, are not reliable.

The Computational Fluid Dynamic (CFD), offers the best alternative to direct measurements as well as analytical models [2].

Recently, have seen the rise of numerical studies on HAWT aerodynamics performed on the full 3D Navier-Stokes models.

The authors Hand, And Fingersh have performed important work on the Unsteady Aerodynamics Experiment Phase VI at the National Renewable Energy Laboratory (NREL) [2, 3]. The authors Sørensen [4] and Johansen [5] performed simulations of the

NREL phase VI rotor with a rotor-fixed reference frame. Also the author Li Y. [6] compared the NREL Phase VI turbine, using unsteady RANS and DES turbulence modeling.

The authors Massouh F. and Dobrev I. have made several numerical and experimental work in the laboratory of ENSAM Paris Tech to explore the wake of the rotor [7, 8].

The auteur N. Troldborg [9], has study of the characteristics of wakes of wind turbines operating in various flow conditions;

In this work, we will present a numerical modeling of the stationary and three-dimensional flow around the rotor in a very wide domain of study, in order to understand the development of the wake of the wind turbine downstream. The computations presented in this paper have been obtained using a finite-volume method by fluent commercial computational fluid dynamic package [10]. The major domain was modeled using the conservation equations for the continuity and Reynolds Averaged Navier Stokes equations using the concept of turbulent viscosity based on SST  $k-\omega$  turbulent model [11].

## 2. Mathematical Model

The mathematical model includes Continuity and Momentum equations. These equations are solved, with the assumption of incompressible and turbulent-steady flow. Basically, they are the incompressible steady-RANS classical equations. The details of these methodologies are not given here. In RANS, only the time-averaged equations are solved, and the fluctuations associated as

Reynolds stresses ( $-\overline{u_i u_j}$ ) are represented by turbulence models Continuity and Momentum equations are

$$\frac{\partial}{\partial x_i} (\tilde{U}_i) = 0 \tag{1}$$

$$\frac{\partial \tilde{U}_i}{\partial t} + \frac{\partial}{\partial x_i} (\tilde{U}_i \tilde{U}_j) = -\frac{1}{\rho} \frac{\partial \bar{P}}{\partial x_i} + \frac{\partial}{\partial x_i} (\bar{\tau}_{ij} - \overline{u_i u_j}) \tag{2}$$

$$\begin{aligned} \bar{\tau}_{ij} &= 2\bar{\mu} \left( S_{ij} - \frac{1}{3} S_{kk} \delta_{ij} \right) \\ &\approx 2\bar{\mu} \left( \tilde{S}_{ij} - \frac{1}{3} \tilde{S}_{kk} \delta_{ij} \right) \end{aligned} \tag{3}$$

**k-ω sst model**

The transport equations for the k and ω are:

$$\begin{aligned} \frac{\partial}{\partial t} (\rho k) + \bar{u}_j \frac{\partial}{\partial x_j} (\rho k) = \\ \tau_{ij} \frac{\partial \bar{u}}{\partial x_j} - \beta^* \rho \omega k \\ + \frac{\partial}{\partial x_j} \left[ (\mu + \sigma_k \mu_t) \frac{\partial k}{\partial x_j} \right] \end{aligned} \tag{4}$$

$$\begin{aligned} \frac{\partial (\rho \omega)}{\partial t} + u_j \frac{\partial (\rho \omega)}{\partial x_j} = \\ \frac{\mu}{\mu_t} \tau_{ij} \frac{\partial \bar{u}}{\partial x_i} - \beta \rho \omega^2 + \frac{\partial}{\partial x_j} \left[ (\mu + \sigma_\omega u_i) \frac{\partial \omega}{\partial x_j} \right] \\ + 2(1 - F_1) \sigma_\omega \frac{1}{\omega} \frac{\partial k \partial \omega}{\partial x_i \partial x_j} \end{aligned} \tag{5}$$

$$S_k = P - \rho \beta^* \omega K \tag{6}$$

$$S_\omega = \alpha \frac{\omega}{K} P - \rho \beta \omega^2 \quad \text{and where } \mu_t = \alpha^* \frac{K}{\omega}$$

**3. Numerical Modeling of the Rotor**

The Figure 1 shows a three-bladed wind turbine, it is a commercial wind turbine i.e. Rutland 503 of the Marlec Company positioned in the wind tunnel ENSAM and digitized.

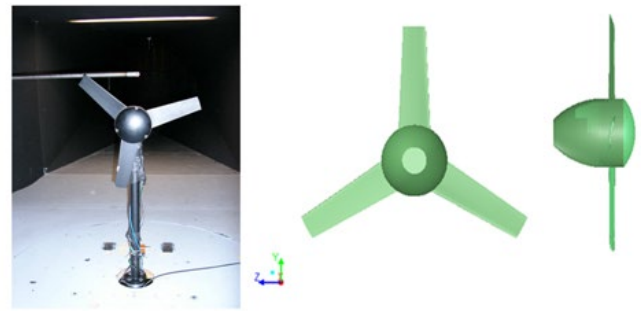


Fig. 1: 3-D Rotor configuration

Table1 presents the geometrical basis parameters of the Rutland rotor. These parameters were taken accurately and digitized for a rotor with the hub. The blades has constant pitch angle. The geometry obtained using these parameters are shows in the figure1.

Table1: parameters of rotor model.

Description	Value
Number of blades	3
Pitch angle	10°
Twist foot of the blade	68 mm
Twist blade tip	48 mm
Diameter hub	135 mm
External diameter	500

**3.1 Calculation Grid**

The calculation grid is done through a 3-D system of coordinates of the actual model of the rotor. In the geometry, the wind turbine tower not included.

The flow field is divided into two mesh areas to take into account the rotation of the rotor

There is an external fluid field and a field which represents the internal fluid of the turbine rotor. So, the domain of computation gathers the mesh of the two zones. Figure 2 shows the mesh elements for the computation model. The dimensions of the field of study are: The diameter of the fluid volume equal to 4.5 R and The length equal to 11R.

These dimensions were selected to have an conform field of study which takes account of the effect of the walls and make it possible to collect all the interactions of the rotor with the healthy flow, which is the wake of the rotor

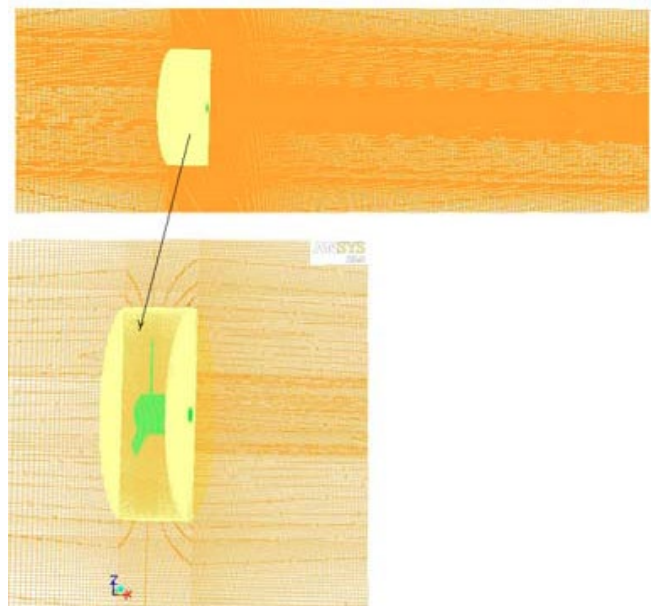


Fig.2: Domain mesh

The geometrical calculation fields defined above were used for the structured grid generation.

Near the rotor blades, the hub and rotor downstream, the meshing is very fine. The cord of blade is divided into 90 intervals, which are refined in the edges. 10 layers of mesh in the vicinity of the blades walls are used in order to improve the grid of the boundary layer. The initial size of the mesh in the normal direction is 0.15 percent of the cord and the growth promoter of 1.25 is used. The mesh fineness near the wall is  $\Delta x = 10^{-4}$  which allows  $y^+ = 30$ .

To account for wake expansion, a high concentration of mesh size has been distributed in the downstream rotor region. The entire domain was divided into 210 blocks. The total number of hexahedral meshes in the study field is about 8 million.

The Frozen Rotor approach is used to define the interface of the two references and to take account of their relative displacement.

### 3.2 Calculation Conditions

The boundary conditions selected for this simulation are the upstream speed and the downstream static pressure. This combination of boundary conditions is physically justifiable. Indeed, the studied wind turbine is intended to receive air with the atmospheric pressure.

The flow is studied with velocity of the wind to 9.3 m/s. The domain of the rotor in rotation simulates the wind rotor I which rotates 1300, 1500 and 1800 rpm.

These values of speed were chosen in reference to experimental work realized in the laboratory of ENSAM [12]. Generally, the tip speed ratio (TSR) is used to analyze the performance of the wind turbine. The TSR is defined by the formula 5:

$$\lambda = \frac{\pi \times N \times D}{60 \times V}$$

D is the rotor diameter and .N is the rotational velocity

## 4. Results and Discussion

### 4.1 Analysis of the Far Wake.

Numerical calculations made it possible to explore the wake of the rotor on a large downstream field, to visualize the vortices emitted from the tip of the blade and the vortex of the hub. Figure 3 clearly illustrates the development of the downstream wake, generating vortices from the blade structure and vortex hub. The wake develops toward the downstream of the rotor model is presented in axial position and at the TSR equal 3.63

The wake zone downstream of the rotor shown is divided by two lines passing through the vortices. Therefore, the downstream flow is divided equally into two parts: an inner part where the axial velocity is slowed by the vortices and an outer part in which the velocity is accelerated by the vortices. The wake of the hub is very bulky therefore; the hub is a source of disturbances and high aerodynamic instability as shown in the figure. This downstream velocity field shows the increase in the diameter of the tube current line caused by the deceleration of the flow created by the wind turbine.

In the inner zone, the generated wake can also be divided mainly into two distinct regions, a near wake and a long wake zone. The near wake is the area just behind the rotor.

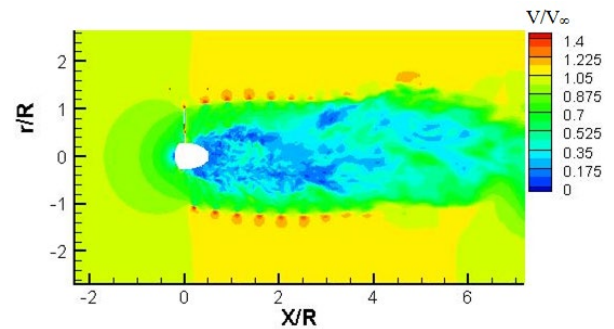


Fig.3: Velocity field around the wind turbine in the vertical plane

In the near wake, there is the central vortex of the hub and the marginal vortices that develop in the tips of the blades. The figure 5 shows the predicted position of the tip vortex. The enlargement of the section is observed in the direction of the wind and from the plane of the rotor.

The far wake is at a distance of approximately four times the radius of the rotor. At this distance, decomposition of the tip vortex occurs and the wake becomes very turbulent with irregular vortex structures.

### 4.2 Wake Rotation

The generation of the helical wake is closely coupled with the blade aerodynamics, strongly influencing the vortex properties [13]. Figure 4 shows the transversal vorticity magnetude in the plane for the turbine wake at  $x/D = 0.1, 0.4, 1.2$  and  $x/D = 1.6$ .

The figure shows the helical wake, the analysis of this result demonstrate that the wake turned faster near the center. The center of rotation corresponds to the axis of rotation of the wind turbine. For the far wake, the center of rotation was located in the axis of rotation and the speed of rotation of the wake decreases this is due to the bursting of the wake.

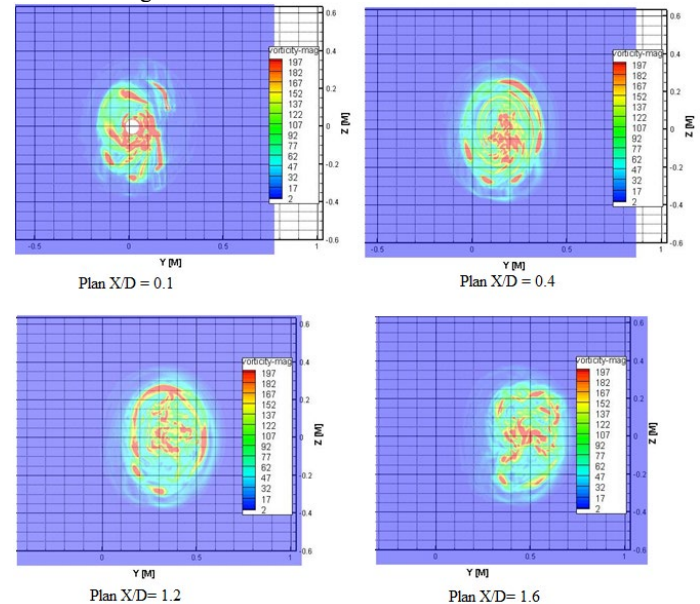


Fig. 4: Vorticity magnetude

### 4.3. Comparison Numerical Results and Experimental Data

Figure 4 shows the comparison of numerical results and experimental measurements in the same position of velocity fields of the near wake. The velocity field that develops downstream of the rotor shows that the positions of the end vortices are located where the velocity varies rapidly in the radial direction.

The tip vortices move with the fluid and they have a helical shape. The investigation plan through these helical tip vortex shows that

the vortex core has a black hole with a high velocity gradient. It should be noted that the review of successive velocity fields over time shows a fluctuation in the position of the vortex nuclei. These results show that in the center of the vortex, the velocity varies with the radius from values close to zero for values well above the speed upstream.

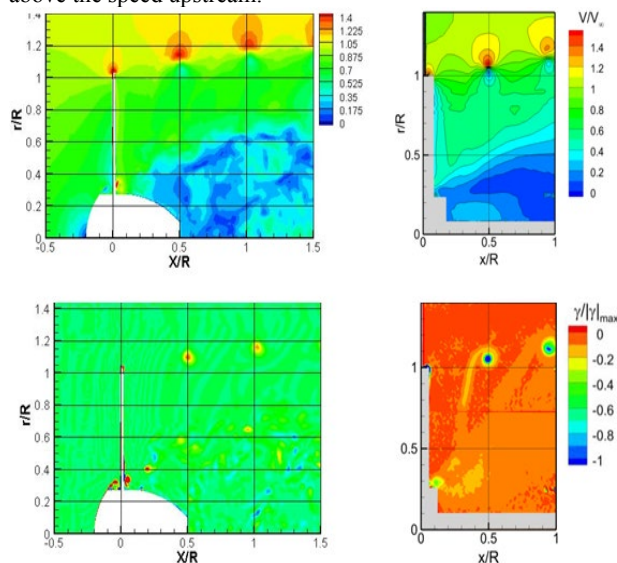


Fig.5: Average velocity (high) and vorticity field (dawn) at  $\lambda = 3.65$ .

## 5. Conclusion

The 3-D numerical simulation has been conducted and results have been compared with the experimental data. In this numerical modelling, a very refined grid has been made which makes it possible to predict the velocity fields near and far the wind turbine rotor. The URANS approach has predicted successfully the behavior of the flow around the rotor under the effect of the variation of the rotation velocity of the wind turbine.

This modeling leads to the access of the unsteady flow morphology. The analysis of the numerical results confirms the complexity of the unsteady flow around the rotor in rotation, thus the shape of the wake downstream from the rotor.

The hub of the rotor is a source of very significant unsteady flow. The marginal tip vortices resulting from the blade tip are the main source of instability. They produce a very complex flow with strong gradients in velocity. These vortices are not located on a cylindrical surface, as supposed by the linear vortex theory.

The downstream wake propagates over a long distance with a speed deficit. Therefore, the downstream wind turbine is found in the free flow of air with a velocity significantly less than that upstream of the wind turbine. As a result, the power losses are significant for one turbine positioned downstream of another.

For large TSR values, the downstream wake propagates a great distance from the wind turbine in the radial and axial directions.

## References

- [1] Barthelme et al. modelling and measuring flow and wind turbine wakes in large wind farms offshore. Riso National Laboratory for Sustainable Energy, Technical University of Denmark 2009.
- [2] Fingersh, L., et al., Wind tunnel testing of NREL's unsteady aerodynamics experiment. In: Proceeding of ASME Wind Energy Symposium., pp. 129 – 135. (2001)
- [3] Hand, M. et al. Unsteady Aerodynamics Experiment Phase VI: Wind Tunnel Test Configurations and Available Data Campaigns. National Renewable Energy Laboratory, NREL. /TP-500-29955. (2011)
- [4] Sørensen, N. et al., Navier–Stokes predictions of the NREL phase VI rotor in the NASA Ames 80 ft\_120ft wind tunnel. Wind Energy. issue 5, 151–169. (2002)

- [5] Johansen, J. et al., Detached-eddy simulation of flow around the NREL phase VI blade. Wind Energy 5, 185–197. (2002)
- [6] Li, Yuwei, et al., CFD simulations of wind turbine aerodynamics. Renewable Energy issue 37, 285–298. (2012)
- [7] Massouh et al. Investigation of wind turbine near wake. Int. Conf. on Jets, Wakes and Separated Flows, ICJWSF 2005, Tobashi, Mie, Japan, 2005.
- [8] Massouh F. et al. . . Exploration and numerical simulation of wind turbine wake; journal ISJAE. 2007
- [9] Troldborg N. et al. thesis" Actuator Line Modeling of Wind Turbine Wakes" Printed in Denmark by DTU-Tryk, ISBN 978-87-89502-80-9-(2008)
- [10] Fluent, Inc., 2005.
- [11] Menter, F. R. Two-Equation Eddy-Viscosity Turbulence Models for Engineering Applications. *AIAA Journal* 32 (8), 1598–1605. (1994)
- [12] Noura B. et al. "Experimental study of yawed inflow around wind turbine rotor" Journal of Power and Energy 226(5) 664–673 IMechE 2012
- [13] Sherry et al. Characterisation of a horizontal axis wind turbines tip and root vortices. *Experiments in fluids* volume 54 issue 3 page 1-1. 2013